arXiv:1302.2466v1 [physics.optics] 11 Feb 2013

Experimental generation of ring-shaped beams with random sources

Salla Gangi Reddy*, **Ashok Kumar**, **Shashi Prabhakar**, **and R. P. Singh**

Physical Research laboratory, Navarangpura, Ahmedabad, India-380 009.
Corresponding author: sgreddy@prl.res.in

Compiled February 12, 2013

We have experimentally reproduced ring shaped beams from the scattered Laguerre-Gaussian and Bessel-Gaussian beams. A rotating ground glass plate is used as a scattering medium and a plano convex lens collects the scattered light to generate ring shaped beams at the Fourier plane. The experimental results are in good agreement with the theoretical results of Mei and Korotkova (Opt. Lett. **38,** 91–93 (2013)). © 2013 Optical Society of America

OCIS codes: 030.1640, 030.6600.

Ring-shaped or dark hollow beams have found applications in guiding cold atoms [1] and trapping of low refractive index particles [2]. Such beams can be generated through multi-mode light wave guides [3], spiral phase plates [4], multi-mode fibers [5] and computer generated holograms (CGH) [6].

Optical vortices or the Laguerre-Gaussian (LG) beams with zero radial index have attracted a great deal of attention due to their applications in optical manipulation, optical communication and quantum information [7, 8]. These beams are recognized with a dark core in their intensity profile and a helical wavefront [9]. We have considered LG beams with zero radial index throughout the paper. Along with the LG beams, Bessel beams owing to their interesting properties of propagation without an apparent spreading due to diffraction have also been a subject of study since more than two decades [10]. Usually in a laboratory the Bessel beams are generated using a Gaussian laser beam and termed as Bessel-Gaussian (BG) beams. In this letter, we demonstrate the generation of ring-shaped beams from the scattered LG and BG beams.

The scattered light of a Gaussian laser beam through a rotating ground glass (RGG) plate can be modeled as a Gaussian Schell-model (GSM) beam [5]. Following a similar argument, the scattered LG and BG beams through the RGG plate can be approximated as Laguerre Gaussian Schell-model (LGSM) beams and Bessel Gaussian Schell-model (BGSM) beams respectively. Recently, the temporal coherence properties of such beams has also been studied [11, 12] and it has been shown that the decay of coherence becomes sharper with increase in the order of LG beam incident on the RGG plate. A similar type of behavior has been observed theoretically in the spatial correlation function of the LGSM and the BGSM beams [13]. It has been stated that the beams having a rotationally symmetric correlation function with zero value on the beam axis can generate a dark core at the far field intensity distribution. Following their theoretical results, we could produce the ring shaped beams from the scattered LG and BG beams.

Our experimental set up for the generation of ring-shaped beams is shown in Fig. 1. An intensity stabilized He-Ne laser beam of maximum power 1 mW and beam waist 0.3 mm is used to generate LG and BG beams. These beams are produced with the computer generated holography technique using a spatial light modulator (SLM). Different computer generated holograms for generating different LG and BG beams are introduced to the SLM through a computer. The required beam is selected with an aperture $A1$, and passed through the RGG plate. The scattered light from the RGG can be approximated as the corresponding Schell-model beam [5] which is focused with a plano convex lens of focal length 10 cm. The images corresponding to the different input beams are recorded with a CCD camera. The SLM is placed at a distance of 59 cm from the laser and the RGG plate is at a distance of 66 cm from the SLM. Lens is kept at a distance of 28 cm from the RGG plate and the CCD camera is placed 30 cm from the lens. Position of the lens is adjusted to get a clear far field intensity distribution for an optimum diameter of the ring shaped beams that could be captured by the CCD camera.

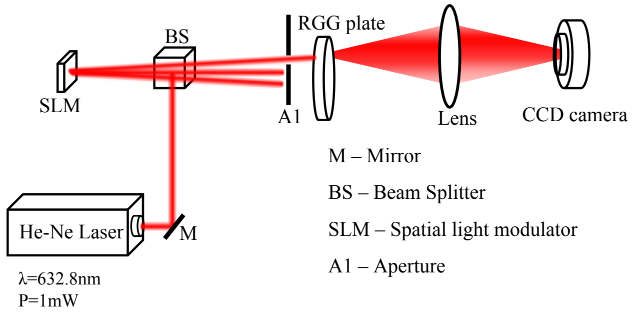

Fig. 1. (Colour online) Experimental set up for the generation of ring shaped beams.

We have recorded the images of scattered second order LG and BG beams having azimuthal index 2 from the static and the rotating ground glass plate at 5 cm away from the plate and also at a distance of 18 cm away from the lens. These images are shown in Fig. 2. One can notice that the recorded images do not show any intensity distribution like original LG and BG beams. The random intensity distributions obtained for static ground glass (Fig. 2(a,b,e,f) gets averaged out in case of the RGG plate (Fig. 2(c,d,g,h)).

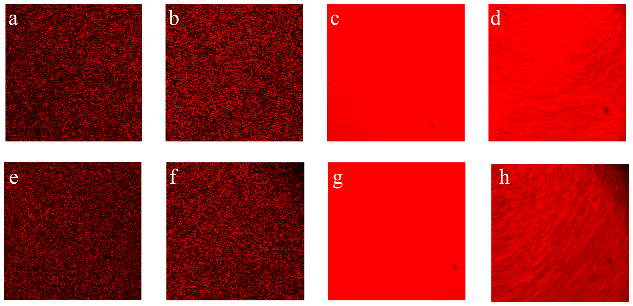

Fig. 2. (Colour online) Images showing the intensity distributions of scattered second order LG (a-d) and BG (e-h) beams; (a, e) are recorded after the ground glass and (b, f) after the lens, while (c, g) and (d, h) are recorded at same places when the ground glass is rotating (linear speed 72.1 cm/sec).

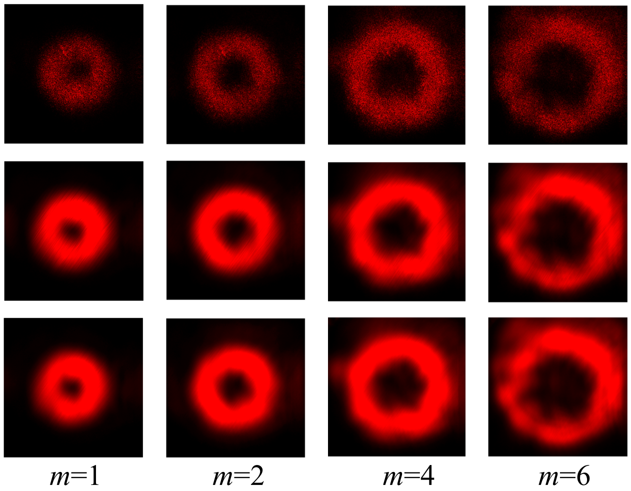

Fig. 3. (Colour online) Far field intensity distribution of the scattered LG beams of different azimuthal indices ($m = 1, 2, 4, 6$) through a static ground glass plate (row 1) and the rotating ground glass plate at different speeds, 72.1 cm/sec (row 2) and 387.9 cm/sec (row 3).

The far field intensity distributions of the scattered LG and BG beams have respectively been shown in Figs. 3 and 4. It could be seen that unlike the random intensity distribution of the scattered light just after the RGG plate or at near field of the lens, the far field intensity distributions form ring shaped beams with dark core for incident beams with nonzero azimuthal index. We have shown the far field intensity distribution for scattered LG and BG beams with their azimuthal indices 1, 2, 4 and 6 (radial index is zero for all images) with a static ground glass plate and also with two different speeds (72.1 cm/sec and 387.9 cm/sec) of the RGG plate. The diameter of the dark core increases with increase in the azimuthal index or order of both LG and BG beams. The dark core remains there if the beam is collimated otherwise it disappears when the beam propagates away from the focus. The experimental results presented in this paper follow the theoretical results of [13].

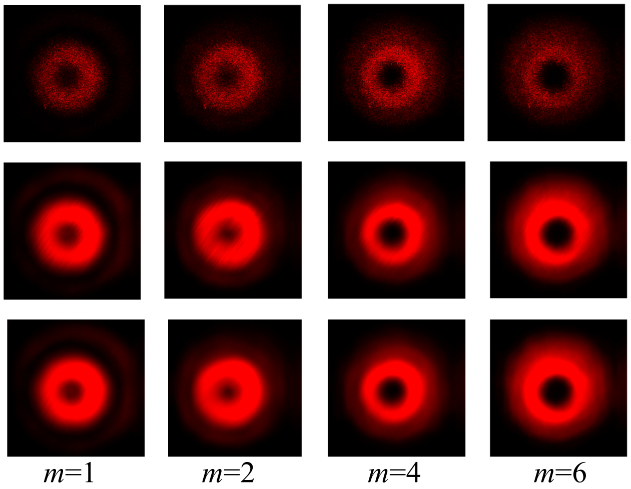

Fig. 4. (Colour online) Far field intensity distribution of the scattered BG beams for same conditions as in Fig. 3

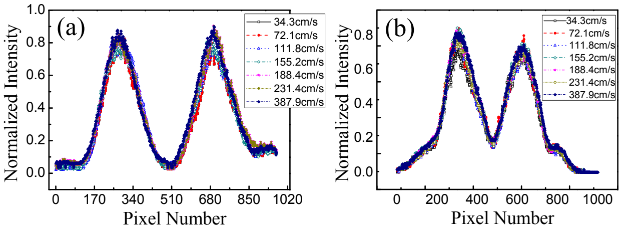

Fig. 5. (Colour online) The line profiles (intensity distribution) along the core of ring shaped beams generated from scattered second order LG (a) and BG (b) beams at different speeds of the RGG plate

Furthermore, we have plotted the line profiles along the dark core of far field intensity distribution of a scattered second order LG and BG beams at different speeds of the RGG plate, shown in Fig. 5. It has been observed that the diameter and the darkness of core is independent of the rotation speeds of the RGG plate. It is well known that the light scattered through a RGG plate can be considered as a partially coherent beam and the degree of coherence can be controlled with the speed of the RGG plate [14]. In the present case, the independence of the size and darkness of core on rotation speed of the

RGG plate indicates that the existence of dark core is independent of the coherence of scattered beam. Although, in the case of partially coherent LG beams, the dark core of the beam disappears when coherence of a given beam is very less [15].

We have also plotted the line profiles through the centers of scattered LG and scattered BG beams of different orders (m = 1-6) at a constant speed 72.1 cm/sec of the RGG plate, shown in Fig. 6. The dark cores of the ring shaped beams are very prominent for non-zero azimuthal index, and as the index increases it becomes broader.

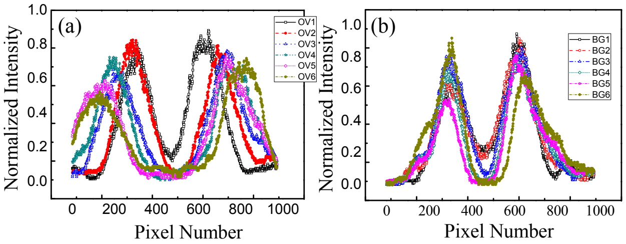

Fig. 6. (Colour online) The line profiles (intensity distribution) along the centers of far field intensity distributions of scattered LG (a) and BG (b) beams for m = 1-6

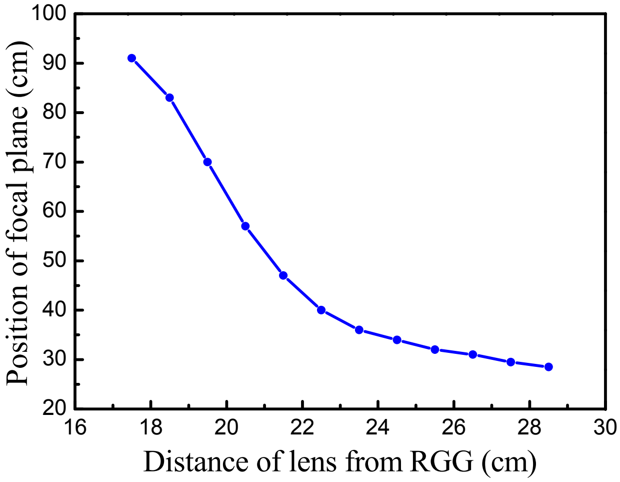

Fig. 7. (Colour online) Plot showing the shifting of focal plane with the position of lens from the RGG plate.

We have also studied the shift in focal plane of the lens when it moves towards or away from the RGG plate. A plot between the position of focal plane (focal shift) and the distance of lens from the RGG plate has been shown in Fig. 7. It is clear that when the lens moves towards the RGG plate, the focal plane shifts away from the lens and vice versa. The similar results have been obtained by changing the aperture size placed in front of the lens for the GSM beams [16]. In both the cases, the focal plane moves towards the lens when we collect less amount of partially coherent light or effectively decrease the aperture size.

We have experimentally generated the ring-shaped beams by collecting the scattered light of LG and BG beams and studied the focal shift for these beams as a function of the amount of light collected by a lens. The generated ring-shaped beams may be of importance in optical trapping experiments. Also the controlled focal shift obtained may be useful in changing the trapping planes. In inverted optical tweezer set up, the focal plane shifts due to the refractive index mismatch between the immersion oil and cover slip [17]; such shifts may be compensated with controlled focal shifts in the path of trapping beams.

References

1. F. K. Fatemi, and M. Bashkansky, Opt. Express. **14,** 4 (2006).
2. K. T. Gahagan, and G. A. Swartzlander, Jr, J. Opt. Soc. Am. B, **15,** 524 (1998).
3. G. Schweiger, R. Nett, B. zel, and T. Weigel1, Opt. Express **18,** 5 (2010).
4. M.W. Beijersbergen, R.P.C. Coerwinke, M. Kristensen, J.P. Woerdman, Opt. Commun. **112,** 321–327 (1994).
5. C. Zhao, Y. Cai, F. Wang, X. Lu, and Y. Wang, Opt. Lett. **33,** 1389–1391 (2008).
6. N. R. Heckenberg, R. McDuff, C. P. Smith, and A. G. White, Opt. Lett. **17,** 221–223 (1992).
7. L. Allen, S. M. Barnett, and M. J. Padgett, *Optical Angular Momentum* (IOP, 2003).
8. G. M. Terriza, J. P. Torres, and L. Torner, Nature Phys. **3,** 305–310 (2007).
9. A. Kumar, P. Vaity, Y. Krishna, and R. P. Singh, Opt. Lasers Eng. **48,** 276 (2010).
10. D. McGloin, and K. Dholakia, Contemp. Phys. **46**, 15–28 (2005).
11. A. Kumar, J. Banerji, and R. P. Singh, Opt. Lett. **35,** 3841–3843 (2010).
12. A. Kumar, J. Banerji, and R. P. Singh, Phys. Rev. A **86,** 013825 (2012).
13. Z. Mei, and O. Korotkova, Opt. Lett. **38,** 91–93 (2013).
14. P. Vaity, A. Kumar, and R P Singh, J. Opt. **15,** 025711 (2013).
15. C. Zhao, F. Wang, Y. Dong, Y. Han, and Y. Cai, Appl. Phys. Lett. **101,** 261104 (2012).
16. F. Wang, Y. Cai, and O. Korotkova, Opt. Commun. **282,** 3408–3413 (2009).
17. K. C. Neuman, E. A. Abbondanzieri, and S. M. Block, Opt. Lett. **30,** 1318–1320 (2005).